Monte Carlo Simulation of the +-J Ising Model with Biquadratic Exchange Interaction

Miyoshi, Yuji
Department of Applied Physics : Graduate Student

Idogaki, Toshihiro
Departmant of Applied Quantum Physics and Nuclear Engineering : Professor

出版情報：九州大学工学紀要. 62 (2), pp.67-83, 2002-06-26. 九州大学大学院工学研究院
バージョン：
権利関係：

Memoirs of the Faculty of Engineering, Kyushu University, Vol. 62, No. 2, June 2002

Monte Carlo Simulation of the $\pm J$ Ising Model with Biquadratic Exchange Interaction

by

Yuji MIYOSHI* and Toshihiro IDOGAKI**

(Received March 25, 2002)

Abstract

The spin-1 $\pm J$ Ising model with uniform biquadratic couplings on simple cubic lattice is studied by the non-equilibrium relaxation and the equilibrium Monte Carlo methods. The reentrant phase transition induced by competition between the bilinear and biquadratic couplings is eliminated gradually with increasing randomness of bilinear couplings and disappears entirely in the strong random system. The dynamic exponent of ferromagnetic transition shows non-universal behavior with changing randomness, while this behavior is not observed in the case of staggered quadrupolar transition.

Keywords: $\pm J$ Ising model, Exchange coupling-biquadratic, Reentrant transition, Phase diagram, Non-equilibrium relaxation, Monte Carlo simulation

1. Introduction

The spin-1 Ising system that contains the bilinear and biquadratic exchange interactions and crystal field is called the Blume-Emery-Griffiths (BEG) model[1], and has been introduced to study the critical and multicritical phenomena associated with physical systems, such as He^3-He^4 mixtures, lattice gases, ternary alloys, metamagnets and multicomponent fluids. Most of the studies on the phase transition of the BEG model have been devoted to the case where the biquadratic coupling constant J' is negative (repulsive) because it may be expected to give a rich phase diagram due to competition between the bilinear and biquadratic couplings. When J' is negative and large enough, it is known that a two-sublattice ordering occurs at low temperatures which is called the staggered quadrupolar (SQ) phase[2–5]. Furthermore, a ferromagnetic (FM) boundary in T-J' phase diagram (T: temperature) exhibits a reentrance in three dimensional lattices ($d = 3$)[2,4].

The inclusion of random frustration of FM and antiferromagnetic (AFM) interactions can have significant effects on the critical properties, *e.g.* appearance of a new ordered phase such as spin glass (SG), reentrant pnenomena, change of the universality class and order of transition. In order to achieve a better understanding of frustrated systems, many

*Graduate Student, Department of Applied Physics

**Professor, Department of Applied Quantum Physics and Nuclear Engineering

infinite-range SG models have been proposed, such as spin-S ($S > 1/2$) Ising, Potts and vector SG models[6–8]. Particularly for the spin-1 Ising SG model with uniform biquadratic couplings, a new SG phase characterized by a two-sublattice structure and reentrant phase transition has been suggested by the replica mean-field approach[9]. In the case of including chemical potential (or crystal field), this model is equivalent to the frustrated BEG model[10–12] which has been introduced to study glass-forming liquids[13,14]. Incorporation of a biquadratic exchange interaction and a chemical potential in glass-forming liquids leads to a characteristic phase diagram with SG transitions of first or second order. However, to our knowledge, none of those works for magnetic and fluid systems addressed the problem of the short-range model in which FM and AFM bilinear couplings have a non-symmetric random distribution.

In this paper, we try to cover significant critical behavior caused by the presence of the biquadratic couplings in the nearest-neighbor-interaction Ising model with the non-symmetric distribution of the bilinear couplings. The spin-1 $\pm J$ Ising model with uniform biquadratic couplings is described by the Hamiltonian

$$\mathcal{H} = -\sum_{\langle i,j \rangle} J_{ij} S_i S_j - J' \sum_{\langle i,j \rangle} S_i^2 S_j^2, \tag{1}$$

where each S_i can take the values 1, 0, or -1. J_{ij} and J' are the nearest-neighbor bilinear and biquadratic coupling constants, respectively. The probability distribution for each bond J_{ij} is given by

$$P(J_{ij}) = p\delta(J_{ij} - 1) + (1 - p)\delta(J_{ij} + 1), \tag{2}$$

where p is the concentration of FM bonds. The system with $p = 1$ is characterized by the FM ordering in the region of $J' > -1$ and the SQ ordering in the region of $J' < -1$, respectively[4] (see Appendix A). The present model corresponds to the system where the FM bond concentration p of the BEG model without the crystal field is extended to $p \leq 1$ (random system), or the system where the spin quantum number S of the $\pm J$ Ising model is extended to $S = 1$ with the inclusion of biquadratic exchange interaction. We are particularly interested in clarifying the following: (i) how the reentrant transition found in the T-J' phase diagram for the pure system is modified by the introduction of randomness; (ii) whether the critical properties of the FM and SQ transitions depend on the biquadratic coupling constant and/or the randomness.

Recently, a new simulation strategy called non-equilibrium relaxation (NER) method, which differs from the standard equilibrium simulations, has been proposed and applied to study disordered system[15–17], quantum-spin system[18,19] and chirality[20]. Furthermore, the NER analysis of fluctuations[21], which is useful technique for estimating both the static and dynamic exponents, was successfully applied to the Ising ferromagnets[22–24]. These NER studies have proved to give an accurate estimation for the critical temperature and exponents while being easily done because the thermal equilibrium state is not necessary to be realized in the simulation, and the size dependence of the NER function is weak even in the critical region. In the case of the SG transition, however, the NER analysis is difficult because the choice of an initial ordered state is neither unique nor straightforward, and the determination of a relaxation function is difficult. So we apply the NER method including the study of the relaxation of fluctuations to the analyses of the FM and SQ transitions, and the equilibrium Monte Carlo (MC) method to the case of the SG transition.

This paper is organized as follows. In §2, we explain the basic concept of the NER and the equilibrium MC methods and show numerical analysis. In §3, the results of the calculations

of the phase diagrams, reentrant phenomena and the critical exponents are presented, as well as the discussion. Final section is devoted to summary.

2. Monte Carlo simulation

2.1 The non-equilibrium relaxation analysis

We define the time-dependent order parameters, $m(t)$ and $q_{\rm s}(t)$, per site, describing the FM and SQ ordering, respectively as

$$m(t) = \langle m'(t) \rangle_{\rm D}, \tag{3}$$

$$q_{\rm s}(t) = \langle q'_{\rm s}(t) \rangle_{\rm D}, \tag{4}$$

with

$$m'(t) = \frac{1}{L^3} \sum_i S_i(t), \tag{5}$$

$$q'_{\rm s}(t) = \frac{2}{L^3} \Big[\sum_{i \in {\rm A}} S_i(t)^2 - \sum_{j \in {\rm B}} S_j(t)^2 \Big], \tag{6}$$

where L is the linear size of lattice, and $\langle \cdots \rangle_{\rm D}$ denotes the ensemble average in terms of the dynamical time evolution, and A and B denote the two interpenetrating sublattices. The kth moment $\mathcal{O}^{(k)}(t)$ of the order parameter $\mathcal{O}(t)$ ($\mathcal{O} \equiv m$ or $q_{\rm s}$) and the time-dependent fluctuation $f_{\mathcal{O}}(t)$ of the order parameter are defined as follows:

$$\mathcal{O}^{(k)}(t) = \langle \mathcal{O}'(t)^k \rangle_{\rm D}, \tag{7}$$

$$f_{\mathcal{O}}(t) = L^3 [\mathcal{O}^{(2)}(t)/\mathcal{O}(t)^2 - 1], \tag{8}$$

where $\mathcal{O}(t)$ and $f_{\mathcal{O}}(t)$ are obtained from the external field h derivative of the free energy F and $\mathcal{O}$, respectively.

For the dynamic relaxation from a completely ordered state, the scaling form of the time-dependent free energy $F(t)$ per site is expected as follows[25,26]:

$$F(t, \tau, h) = t^{-d/z_{\mathcal{O}}} \bar{F}(t^{1/z_{\mathcal{O}}\nu_{\mathcal{O}}} \tau, t^{(d-\beta_{\mathcal{O}}/\nu_{\mathcal{O}})/z_{\mathcal{O}}} h), \tag{9}$$

where

$$\tau = \frac{T - T_{\rm c}}{T_{\rm c}}, \tag{10}$$

is the reduced temperature normalized by the critical temperature $T_{\rm c}$, and $\beta_{\mathcal{O}}$, $\nu_{\mathcal{O}}$ and $z_{\mathcal{O}}$ are the static exponents related to the order parameter and the correlation length, and the dynamic exponent, respectively. At the critical point, the order parameter and the fluctuation obey the power-law behaviors

$$\mathcal{O}(t) \sim t^{-\lambda_{\mathcal{O}}}, \tag{11}$$

$$f_{\mathcal{O}}(t) \sim t^{\lambda_{f\mathcal{O}}}, \tag{12}$$

where $\lambda_{\mathcal{O}}$ and $\lambda_{f\mathcal{O}}$ are called the NER exponent of the order parameter and the NER exponent of the fluctuation, respectively. The exponents reveal the relations

$$\lambda_{\mathcal{O}} = \beta_{\mathcal{O}}/z_{\mathcal{O}}\nu_{\mathcal{O}}, \tag{13}$$

$$\lambda_{f\mathcal{O}} = d/z_{\mathcal{O}}. \tag{14}$$

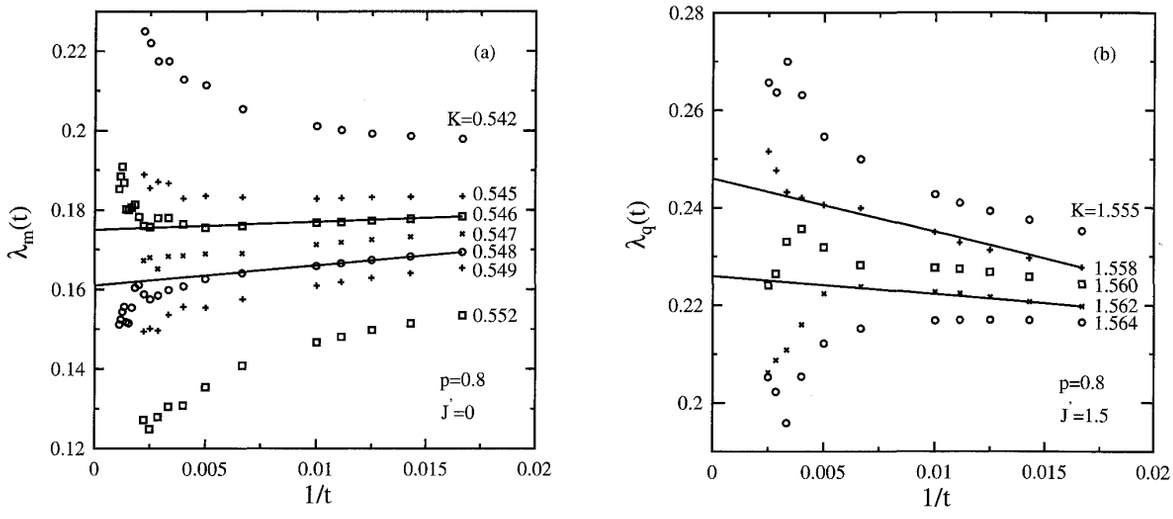

Fig. 1 Inverse time dependence of the local exponents $\lambda_m(t)$, $\lambda_q(t)$ for the random system ($p = 0.8$) when (a) $J' = 0$ and (b) $J' = -1.5$.

The order parameter $\mathcal{O}(t)$ decays exponentially to zero in the paramagnetic (PM) phase, and to a non-zero value in the ordered phase. In order to determine the critical point, we observe the local exponent $\lambda_{\mathcal{O}}(t)$ related to the order parameter as

$$\lambda_{\mathcal{O}}(t) = -\frac{\mathrm{dlog}\, \mathcal{O}(t)}{\mathrm{dlog}\, t}. \tag{15}$$

This local exponent $\lambda_{\mathcal{O}}(t)$ goes to infinity in the PM phase and to zero in the ordered phase. It goes to the NER exponent $\lambda_{\mathcal{O}}$ at the critical point.

The local exponent $\lambda_{\mathcal{O}}(t)$ is estimated by the least square fitting of $\log \mathcal{O}(t)$ against $\log t$ over appropriate time interval around each t. In order to determine the critical exponents, we also estimate the NER exponent of the fluctuation $\lambda_{f\mathcal{O}}$ at the critical point. The NER exponent of the fluctuation is derived by the least square fitting of the slopes of the curves in a $\log f_{\mathcal{O}}$-$\log t$ plane. The critical exponents $\beta_{\mathcal{O}}/\nu_{\mathcal{O}}$ and $z_{\mathcal{O}}$ can be evaluated from $\lambda_{\mathcal{O}}$ and $\lambda_{f\mathcal{O}}$ by using Eq.(13) and Eq.(14).

The NER simulations are performed on simple cubic lattice of $100 \times 100 \times 100$, which is large enough to prevent the finite-size effect (see Appendix B), with periodic boundary condition. The simulation parameters used are given as follows: the maximum time of the simulations $t_{\max}$ = 500-1000 MC steps per spin (see Appendix B); the number of bond samples N_{s} = 1600-3200. Starting from the initial spin configuration $(S_A, S_B) = (1, 1)$ for the case of the FM transition and $(S_A, S_B) = (1, 0)$ for the case of the SQ transition, the system is updated by the heat-bath single spin-flip algorithm. We used the sequential sampling along each of the two sublattices which is useful in vectorized and parallelized calculations (see Appendix C).

The inverse time dependence of the local exponents $\lambda_m(t)$, $\lambda_q(t)$ is shown in **Fig. 1** for the random system ($p = 0.8$) when (a) $J' = 0$ and (b) $J' = -1.5$. In **Fig. 1** (a), the curves of the local exponents $\lambda_m(t)$ turn up when $1/t$ goes to zero for the inverse temperature $K = 1/T \leq 0.546$, and the curves turn down for $K \geq 0.548$. Therefore the critical point exists in $0.546 < K_{\mathrm{c}} < 0.548$, and we conclude that $K_{\mathrm{c}} = 0.547(1)$. The curve of the local exponent for $K = 0.546$ (lower limit of K_{c}) is extrapolated to 0.175 for $t \to \infty$ when we

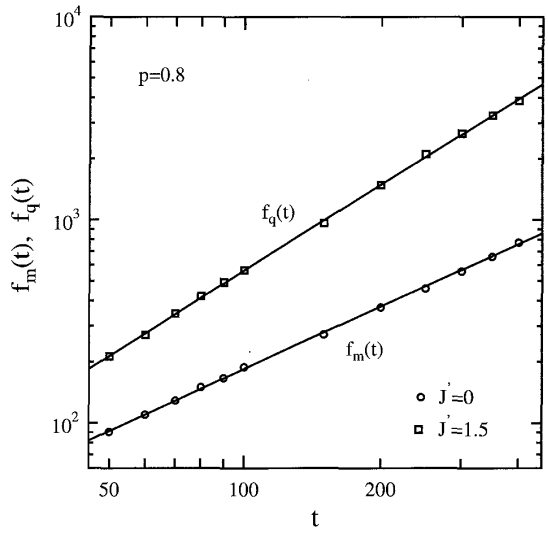

Fig. 2 Time evolution of the fluctuations $f_m(t)$, $f_q(t)$ at the critical temperature for the random system ($p = 0.8$) when $J' = 0$ and $J' = -1.5$.

neglect the final turn-up. The curve of the local exponent for $K = 0.548$ (upper limit of K_c) is extrapolated to 0.161 for $t \to \infty$ when we neglect the final turn-down. Then we conclude that $\lambda_m = 0.168(7)$. From **Fig. 1** (b), similar analysis gives $K_c = 1.560(2)$ and $\lambda_q = 0.236(10)$ for the SQ transition.

At the critical temperature, the time evolutions of the fluctuations $f_m(t)$, $f_q(t)$ of the order parameters are plotted in log-log scale in **Fig. 2** for the random system ($p = 0.8$), when $J' = 0$ and $J' = -1.5$. The values of the critical temperature are $K_c = 0.547$ for $J' = 0$, and $K_c = 1.56$ for $J' = -1.5$. The curves obey the asymptotic power-law behavior for both of the FM ($J' = 0$) and SQ ($J' = -1.5$) phase transitions. As the slopes of the curves, we obtain 1.04 for $K = 0.546$ (lower limit of K_c) and 0.991 for $K = 0.548$ (upper limit of K_c) in the system with $p = 0.8$ and $J' = 0$. Then we conclude that $\lambda_{fm} = 1.02(3)$. From the behavior of $f_q(t)$ in **Fig. 2**, we obtain $\lambda_{fq} = 1.40(5)$ for the SQ transition with $p = 0.8$ and $J' = -1.5$.

Similar analyses made in **Fig. 1** and **Fig. 2** are performed for various combinations of p and J'. The results of the critical temperature and NER exponents $\lambda_{\mathcal{O}}$, $\lambda_{f\mathcal{O}}$ are listed in **Table 1** and **Table 2**, for the FM and SQ transitions, respectively. In the FM transition, the NER exponents λ_m, λ_{fm} become smaller when the concentration p becomes lower for the systems with the same value of J', and this behavior of λ_m coincides with the previous result on the spin-1/2 system[15]. The critical temperature and the NER exponents λ_q, λ_{fq} of the SQ ordering are independent of the concentration p for the systems with the same value of J'.

2.2 The equilibrium Monte Carlo analysis

In order to determine the complete phase diagrams, we estimated the SG critical temperature in the extended region by using the Binder's fourth-order cumulant[27], which becomes independent of L at the critical point:

$$g_Q = \frac{1}{2}\left[3 - \frac{\langle\langle Q^4\rangle\rangle_c}{\langle\langle Q^2\rangle\rangle_c^2}\right], \tag{16}$$

Table 1 The critical temperature and the NER exponents for the FM transition. H (or L) corresponds to the cases for higher (or lower) critical temperature in the reentrant region.

		$S=1$				$S=1/2$
p	J'	K_c	$T_c=1/K_c$	λ_m	λ_{fm}	λ_m
1	0	0.31288(8)	3.1962(8)	0.25(1)	1.47(2)	0.248(1)[23]
	−0.5	0.4126(1)	2.4237(6)	0.250(8)	1.47(2)	
	−0.95	0.7803(8)	1.282(1)	0.240(13)	1.40(4)	
	-1.02^{H}	1.115(3)	0.897(2)	0.248(12)	1.45(6)	
	-1.02^{L}	4.01(1)	0.2492(8)	0.247(7)	1.43(3)	
0.9	0	0.3918(2)	2.553(1)	0.23(1)	1.34(3)	0.23(1)[15]
	−0.5	0.5543(3)	1.8042(8)	0.231(5)	1.35(1)	
	−0.95	2.108(8)	0.475(2)	0.228(11)	1.37(2)	
0.8	0	0.547(1)	1.828(3)	0.168(7)	1.02(3)	0.16(1)[15]
	−0.5	0.863(3)	1.159(3)	0.163(9)	1.00(3)	
	−0.95	7.25(5)	0.138(1)	0.161(9)	0.95(3)	

Table 2 The critical temperature and the NER exponents for the SQ transition.

p	J'	K_c	$T_c=1/K_c$	λ_q	λ_{fq}
1	−1.1	7.40(1)	0.1351(2)	0.236(6)	1.414(5)
	−1.5	1.564(2)	0.6396(6)	0.237(7)	1.44(3)
0.8	−1.1	7.365(5)	0.13578(9)	0.237(5)	1.44(2)
	−1.5	1.560(2)	0.6410(8)	0.236(10)	1.40(5)
0.5	−1.1	7.37(2)	0.1358(3)	0.232(12)	1.42(2)
	−1.5	1.559(2)	0.6416(6)	0.239(7)	1.44(1)

where $\langle\cdots\rangle$ and $\langle\cdots\rangle_{\mathrm{c}}$ denote thermal average for a given set of bonds and configurational average for various sets of bond distribution, respectively. The SG order parameter Q is defined by the overlap between the two independent replicas 1 and 2 with the same set of bonds[28,29]:

$$Q=\frac{1}{L^3}\sum_i S_i^{(1)}S_i^{(2)}. \tag{17}$$

After t_0 MC steps per spin for equilibration, an additional $2t_0$ MC steps per spin are carried out for thermal average. The simulation parameters used for the Binder cumulant analysis are given as follows: the linear size of lattice L = 4-16; the largest time for equilibration $t_0 = 8\times10^6$ MC steps per spin; the number of bond samples N_{s} = 32-5120.

The size and temperature dependences of g_Q with p = 0.5 are shown in **Fig. 3** for the cases of J' = 0 and −0.5. The curves of g_Q for different sizes clearly fan out at high temperatures, while this is not so clear at low temperatures as well as for the case of spin-1/2 system[28]. From the intersection point of those curves, we have estimated T_{c} as 1.0 and 0.6 for J' = 0 and −0.5, respectively. Similar analyses made in **Fig. 3** are performed for various

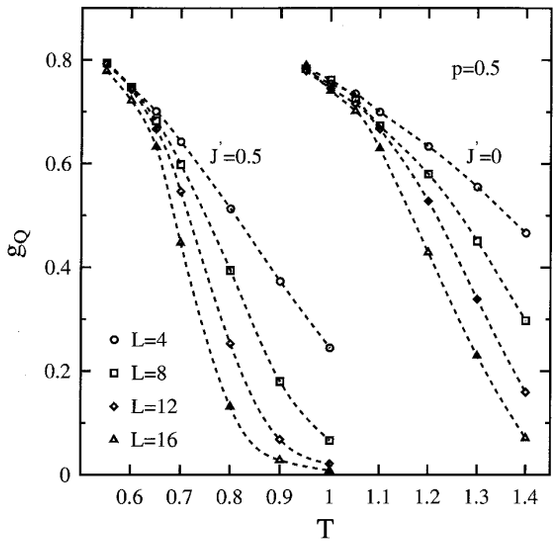

Fig. 3 Temperature dependence of the Binder cumulant g_Q for the SG system ($p = 0.5$) with $J' = 0$ and -0.5.

combinations of p and J'.

3. Results and discussion

3.1 Phase diagrams

The T-J' phase diagram obtained is shown in **Fig. 4** for (a) $p = 1$, 0.9 and 0.8, and (b) is the magnified one at $J' \simeq -1$. Since no clear p-dependence of the critical temperature can be found for the SQ transition (see **Table 2**), the SQ phase boundary is indicated only for the case of $p = 1$. The error bars of the critical temperatures are within the marks' sizes. In the pure and random systems, the phase boundary lines FM-PM and PM-SQ are close to each other at low temperatures and meet at the boundary point $(J', T) = (-1, 0)$. For the pure system, the reentrant phenomenon (PM $\rightarrow$ FM $\rightarrow$ PM) appears in the region $-1.035 < J' < -1$, and this behavior is consistent with the previous result[4]. The present results suggest that the reentrant phenomenon is gradually eliminated with the decrease of p and entirely disappears for the strong random system in the region of $p \leq 0.95$. It is also noted that, for the SG system with $p = 0.5$, the PM-SG phase boundary does not show the reentrant behavior.

In **Fig. 5**, the T-p phase diagram is shown for $J' = 0.5$, 0, -0.5 and -0.95 together with the results for the spin-1/2 system[15,17] and the Nishimori-line[30]: $\exp(2K_{\mathrm{N}}) = p/(1-p)$. The critical temperature $T_{\mathrm{c}}(S)$ of the spin-S system is normalized by the spin quantum number, namely $T_{\mathrm{c}} = T_{\mathrm{c}}(S)/S^2$. Irrespective of the value J', the FM transition temperature decreases with the concentration p or with the increase of randomness. However, the tendency of the decrease is evidently different between the case of $J' = -0.95$ and the other cases of $J' = 0.5$, 0 and -0.5. The T_{c} for the latter cases decrease linearly with p but the curve for $J' = -0.95$ shows especially rapid and large reduction in the region of $0.9 < p < 1$. This extraordinary reduction of T_{c} reflects the reentrant phenomena explained in the T-J' phase diagram.

By the use of the gauge theory, it has been proved that the critical concentration p_0 of

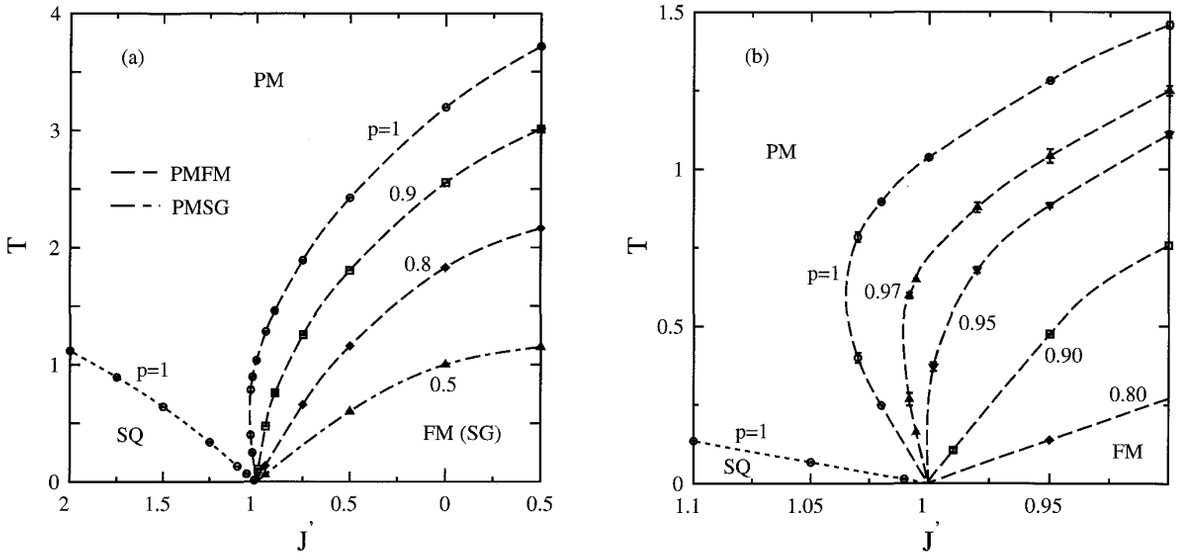

Fig. 4 T-J' phase diagrams for (a) $p = 1$, 0.9 and 0.8, (b) $p = 1$, 0.97, 0.95, 0.9 and 0.8; (b) is the magnified picture at $J' \simeq -1$.

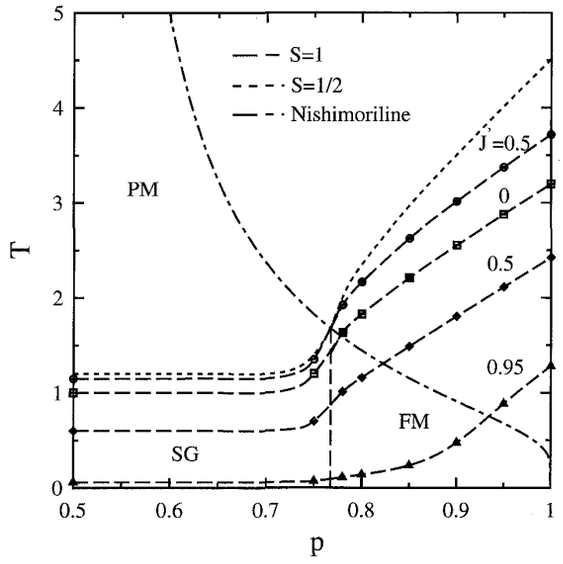

Fig. 5 T-p phase diagram for $J' = 0.5$, 0, -0.5 and -0.95 together with the spin-1/2 results. The dashed curve shows the Nishimori-line.

FM bonds, below which no FM phase exists, for a $\pm J$ non-Ising model is equal to or larger than p_0 for the spin-1/2 $\pm J$ Ising model on the same lattice[31]. The same type of argument can easily apply to the $\pm J$ spin-1 Ising model including the biquadratic exchange interaction and the crystal field. The local gauge transformation leads to the following relation for the FM correlation function,

$$|\langle\langle S_0 S_r\rangle_K\rangle_c| \leq \langle|\langle\sigma_0\sigma_r\rangle_{K_N}|\rangle_c, \tag{18}$$

where $\langle\cdots\rangle_K$ denotes the thermal average at inverse temperature K. The variables $\sigma_i(=\pm 1)$ are Ising spins introduced by the gauge transformation. From Eq.(18) and the spin-1/2 result[30], we can prove exactly that the critical concentration of the present spin-1 system

is not smaller than that of the $\pm J$ spin-1/2 Ising model:

$$p_0(S=1) \geq p_0(1/2). \tag{19}$$

Furthermore, it has been argued that a geometry-induced phase transition by the frustration distribution of bond confugurations $\{J_{ij}\}$ exists at asymmetric distribution of FM and AFM bonds[32]. This geometric anomaly which is independent of the spin variables, suggests a vertical phase boundary separating the FM and the non-FM phases. Assuming the vertical boundary in the spin-1/2 system, the critical concentration $p_0(1/2)$ is believed to be equal to the concentration $p_{\rm mc}(1/2) = 0.7673(3)$[17] at the multicritical point where the PM, FM and SG merge. In the present model, it is considered that the biquadratic exchange interaction does not affect the geometric anomaly, so the vertical boundary occurs at the multicritical concentration of the spin-1/2 system: $p = p_{\rm mc}(S=1/2) = 0.7673(3)$.

3.2 Reentrant phenomena

The NER method suggests that the reentrant phenomena occur at $J' \simeq -1$ where the interactions between J_{ij} and J' are strongly frustrated for the weak random system in the region $0.95 < p \leq 1$. In this section, we examine the behavior of the thermal quantities in the reentrant region and discuss its physical background together with the stability of the ordered phase.

By using the equilibrium simulation, we calculated the order parameters m, $q_{\rm s}$ and the specific heat C per site, defined as

$$C = \frac{\langle\langle E^2\rangle\rangle_{\rm c} - \langle\langle E\rangle^2\rangle_{\rm c}}{L^3T^2}, \tag{20}$$

where E denotes the system internal energy. The temperature dependences of m, $q_{\rm s}$ and C around the region of reentrant transition are shown in **Fig. 6** and **Fig. 7**, respectively, for (a) the pure system ($p = 1$) and (b) the random system ($p = 0.97$). Reentrant transition arises in the region $-1.035 < J' < -1$ for the system with $p = 1$, and in $-1.011 < J' < -1$ for the system with $p = 0.97$. The calculations are performed for the central values of the reentrant region: $J' = -1.02$ for $p = 1$, and $J' = -1.005$ for $p = 0.97$. From the the temperature dependence of $q_{\rm s}$ in **Fig. 6**, the SQ phase transition is confirmed to occur at extremely low temperature and to be second-order transition. The saturated value of m is small, compared with that of $q_{\rm s}$ which is about 2/3.

The specific heat of reentrant transition in the pure system has a weak cusp at both high and low temperatures (**Fig. 7** (a)). This cusp becomes weaker gradually with decreasing the value of J'. In the previous MC simulation for the pure system[4], it has been reported that the specific heat shows no singularity for the reentrant phase transition. This contradiction will be explained as follows: their calculations has been performed at $J' = -31/30 = -1.03\dot{3}$, and this value is too close to the lower boundary value of the reentrant region $-1.035 < J' < -1$ to check such weak singularity. In practice, the anomaly of the specific heat associated with the reentrant transition is so weak that it is broadened and almost eliminated even by the effect of small randomness (**Fig. 7** (b)).

The origin of the reentrant transition can be traced back to competition between the bilinear and biquadratic couplings. In order to obtain clear insight of this reentrant phenomena, we have looked into the spin configurations at different temperatures. **Fig. 8** shows snapshots for the pure system ($p = 1$) with $J' = -1.02$. Solid circles, open circles and vacancies represent spins of $S_i = 1, -1, 0$, respectively. The system is in the PM phase at $T = 1.5$ (a), the FM phase at $T = 0.5$ (b), the reentrant PM phase at $T = 0.1$ (c) and the SQ phase

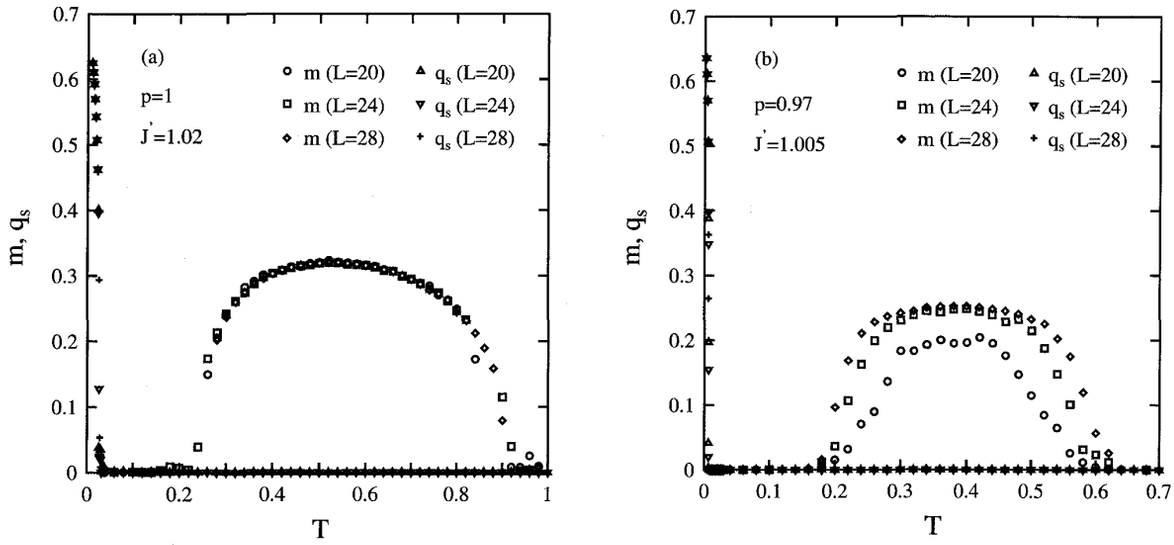

Fig. 6 Temperature dependence of the order parameters m, q_s for (a) the pure system ($p = 1$) with $J' = -1.02$ and for (b) the random system ($p = 0.97$) with $J' = -1.005$.

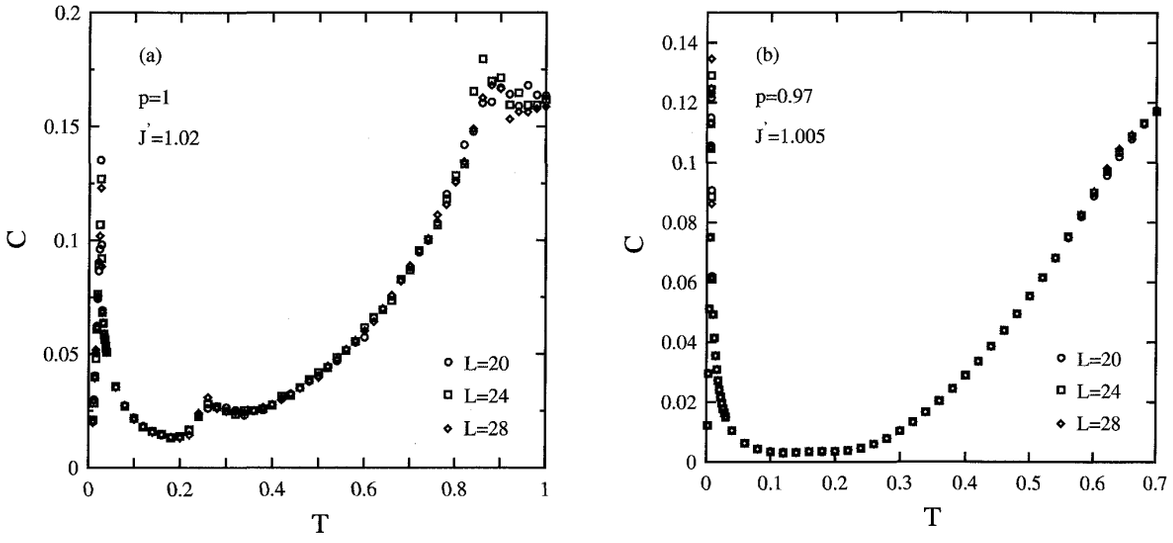

Fig. 7 Temperature dependence of the specific heat C for (a) the pure system ($p = 1$) with $J' = -1.02$ and for (b) the random system ($p = 0.97$) with $J' = -1.005$.

at $T = 0.01$ (d). In the region of $J' < -1$, the internal energy favors the nearest-neighbor spin pairs involving $S_i = 0$: $(S_i, S_j) = (0, 1)$, $(0, 0)$ and $(0, -1)$ (the orthogonal-spin pair), leading the SQ ordering at low temperatures. Also, in the present system of $p = 1$, the bilinear exchange interaction tends to prefer the parallel-spin pairs $(S_i, S_j) = (1, 1)$ and $(-1, -1)$ to other kinds of spin pairs. With decreasing temperature from the PM state (**Fig. 8** (a)), the parallel-spin pairs increase gradually, decreasing the antiparallel-spin pairs $(S_i, S_j) = (1, -1)$, and form weak FM long-range order (**Fig. 8** (b)). It should be noted here that this FM long-range order is so weak that we cannot find any percolating network within a single plane. This is consistent with the previous result that the reentrant

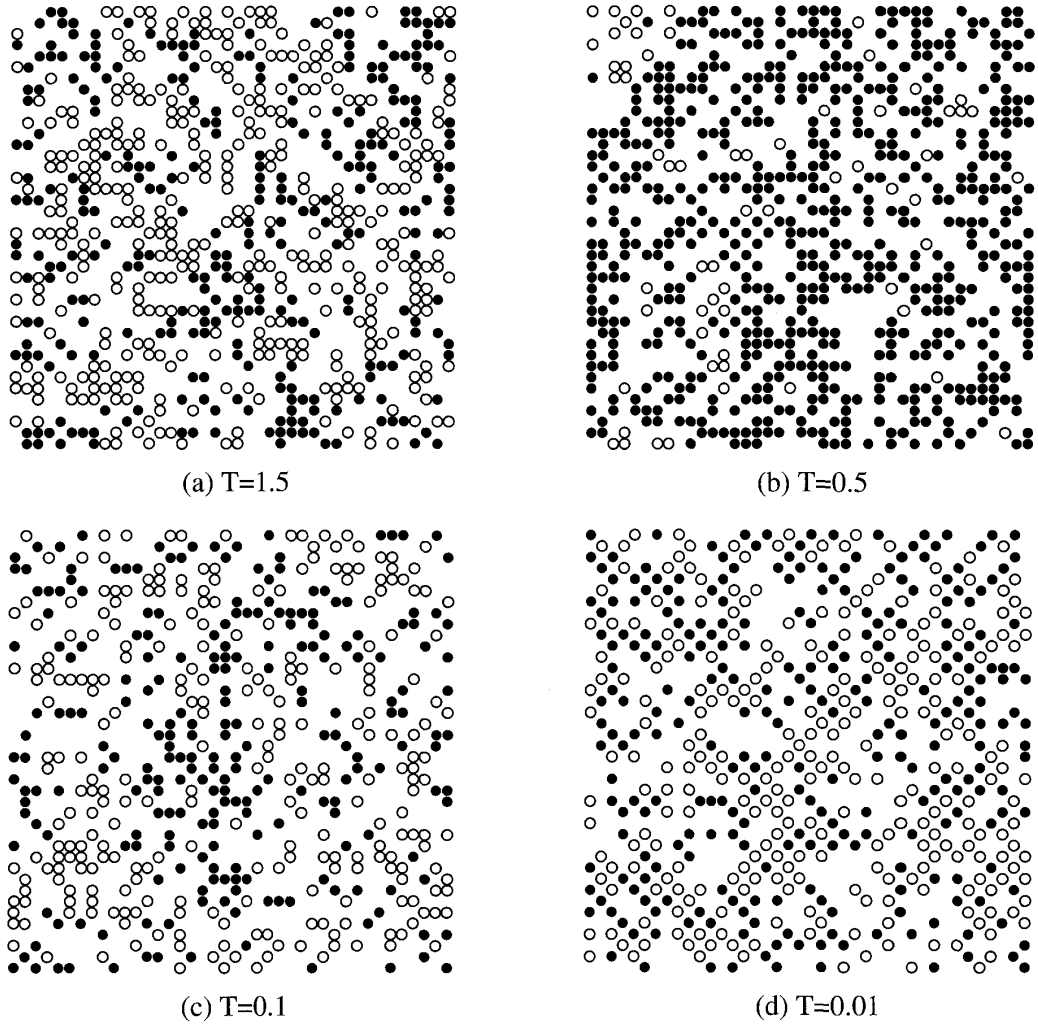

Fig. 8 Spin configuration for the pure system ($p = 1$) with $J' = -1.02$ at (a) $T = 1.5$, (b) 0.5, (c) 0.1 and (d) 0.01.

phenomena do not occur in two-dimensional lattice [3] and also with the present result that, even in three-dimensional lattice, the decrease of p eliminates the reentrant transition. With further cooling, the increase of the number of the orthogonal-spin pairs overcomes that of the parallel-spin pairs, and this again leads to the PM state at low temperatures (**Fig. 8** (c)). In **Fig. 8** (c), we can see that the number of the antiparallel-spin pairs is significantly decreased, and the FM parallel-spin clusters are isolated by spins $S_i = 0$. With further cooling, the SQ state having the regular two-sublattice arrangement of the orthogonal-spin pairs appears at very low temperatures and is stable down to the absolute zero temperature (**Fig. 8** (d)).

In order to confirm the stability of the FM and also SQ phases in the reentrant region, the time evolution of the order parameter when equilibration starts from different initial configurations: (a) ferromagnetic (FMIC) and random (RIC) one, and (b) staggered quadrupolar (SQIC) and RIC is calculated (**Fig. 9**). The simulations are performed for (a) the FM phase at $T = 0.4$ in the random system ($p = 0.97$) with $J' = -1.005$, and for (b) the SQ phase at $T = 0.02$ in the pure system ($p = 1$) with $J' = -1.02$. The linear size of lattice is $L = 18$, and the number of bond samples is $N_s = 320$. Time evolution from SQIC corresponds to the heating process, and the case of RIC corresponds to the cooling process. It is suggested that,

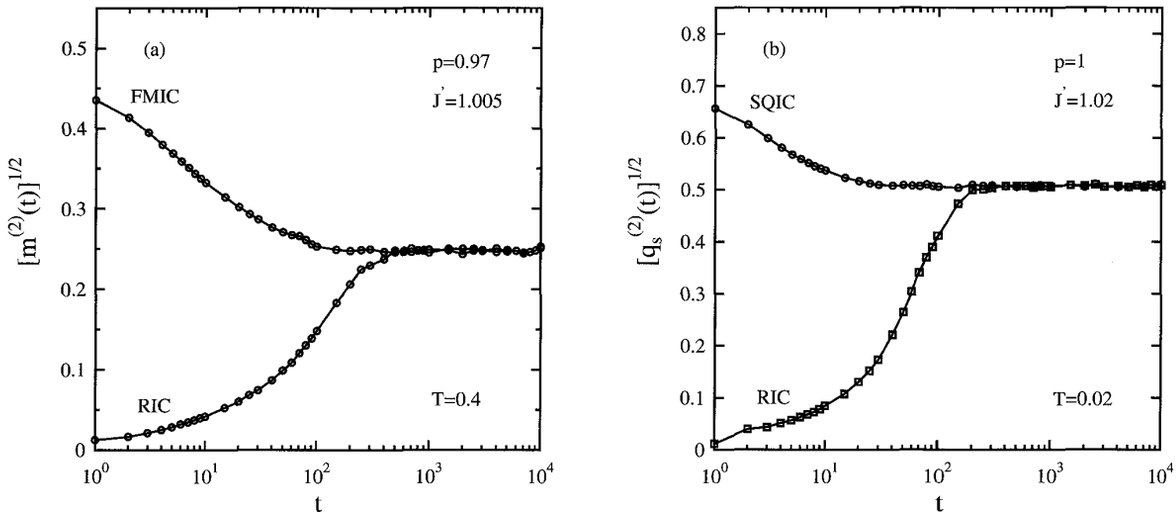

Fig. 9 Time evolution of the order parameter when equilibration starts from different initial configurations: (a) FMIC and RIC, and (b) SQIC and RIC. The simulations are performed for (a) the FM phase in the random system ($p = 0.97$) with $J' = -1.005$, and for (b) the SQ phase in the pure system ($p = 1$) with $J' = -1.02$.

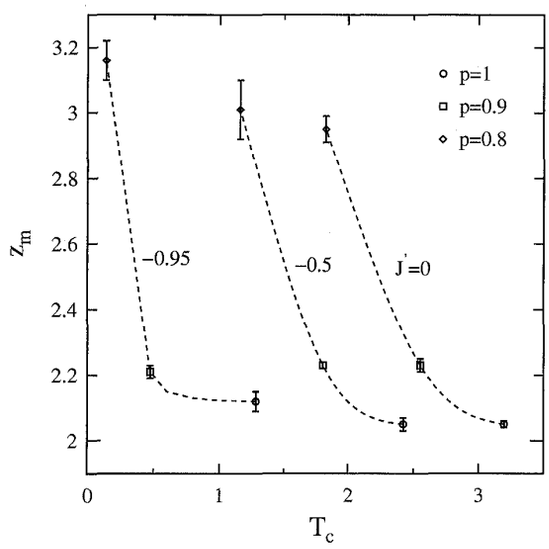

Fig. 10 Critical temperature T_c dependence of the dynamic exponent z_m for $J' = 0$, -0.5 and -0.95.

irrespective of the initial condition, each order parameter becomes stabilized after sufficient relaxation time for this parameter region and hysteresis does not occur. Similar analyses are performed for other region of parameter (p, J'), and it is confirmed that the present phase transitions of finite temperatures in all region are the second-order transition.

3.3 Critical exponents

Finally, we discuss the critical exponents $\beta_{\mathcal{O}}/\nu_{\mathcal{O}}$, $z_{\mathcal{O}}$ obtained from $\lambda_{\mathcal{O}}$ and $\lambda_{f\mathcal{O}}$ given in **Table 1** and **Table 2**. These exponents are summarized in **Table 3** and **Table 4** for

Table 3 The critical exponents at the FM transition. H (or L) corresponds to the cases for higher (or lower) critical temperature in the reentrant region. $*$ denotes the results of the spin-1/2 system.

		present		previous	
p	J'	β_m/ν_m	z_m	β_m/ν_m	z_m
1	0	0.510(13)	2.04(3)	$*0.517(2)$[22]	$*2.042(6)$[22]
	-0.5	0.510(9)	2.04(3)		$*2.055(10)$[23]
	-0.95	0.515(14)	2.15(6)		
	-1.02^{H}	0.513(2)	2.07(9)		
	-1.02^{L}	0.517(5)	2.10(4)		
	$-31/30^{\mathrm{H}}$	-	-	0.511(13)[24]	2.05(9)[24]
	$-31/30^{\mathrm{L}}$	-	-	0.509(15)[24]	2.02(8)[24]
0.9	0	0.513(11)	2.23(5)	$*0.55(5)$[34]	
	-0.5	0.512(7)	2.22(2)		
	-0.95	0.499(16)	2.19(4)		
0.8	0	0.496(8)	2.95(7)		
	-0.5	0.490(13)	3.01(9)		
	-0.95	0.508(12)	3.16(10)		

Table 4 The critical exponents at the SQ transition.

		present		previous	
p	J'	β_q/ν_q	z_q	β_q/ν_q	z_q
1	$-31/30$	-	-	0.513(17)[24]	2.07(9)[24]
	-1.1	0.501(11)	2.122(7)		
	-1.5	0.496(5)	2.09(4)		
0.8	-1.1	0.495(5)	2.09(2)		
	-1.5	0.506(3)	2.15(8)		
0.5	-1.1	0.489(17)	2.11(4)		
	-1.5	0.499(10)	2.09(2)		

the FM and SQ transitions, respectively. In the pure system, it is considered that the critical exponents β_O/ν_O, z_O of the FM and SQ transitions are consistent with the results of the BEG model[24], and belong to the spin-1/2 Ising universality class, independent of J'. According to the Harris criterion[33], for simple cubic lattice, it is conjectured that the critical phenomena at the FM transition in the disordered system are different from those in the pure system. At the modest scale of our simulation, however, this conjecture cannot be decisively answered although the static exponent β_m/ν_m in the system with $p = 0.8$ seems to be slightly smaller than that in the pure system. The static exponents β_q/ν_q of the SQ transition in the random system seem to obey the spin-1/2 Ising universality class, independent of p.

The critical temperature T_c dependence of the dynamic exponent z_m is shown in **Fig. 10** for the system with $J' = 0$, -0.5 and -0.95. The error bars of T_c are negligibly small compared with those of z_m. It is found that z_m increases monotonously with decreasing the

concentration p and shows non-universal behavior. Regarding the dynamic exponents at the FM and SQ transitions, our results suggest that z_m and z_q belong to different universality classes in the random system.

4. Summary

We have studied effects of the biquadratic exchange on the phase diagrams of the spin-1 $\pm J$ Ising model on simple cubic lattice. The reentrant phenomenon in T-J' phase diagram observed for the pure system is gradually eliminated with decreasing the concentration p and disappears in the strong random system. It seems that the FM phase in the reentrant region forms a weak long-range order, and the reentrant PM phase is such a kind of phase that does not involve antiparallel-spin pairs. In contrast to the mean-field SG model, there are no possibility of first-order transition and no occurrence of the SG phase with two-sublattice structure. It has been revealed that the dynamic exponent of the FM transition shows non-universal behavior with decreasing p, and the dynamic exponents at the FM and SQ transitions belong to different universality classes in the random system.

Acknowledgements

The simulations were made using the vector-parallel supercomputer Fujitsu VPP700/56.

Appendix I. Degenerated region of the BEG model

The Hamiltonian of the BEG model is described by

$$\mathcal{H} = -\sum_{\langle i,j \rangle} S_i S_j - J' \sum_{\langle i,j \rangle} S_i^2 S_j^2 - D \sum_i S_i^2, \tag{21}$$

where D is the crystal field. The ground state phase diagram is shown in **Fig. 11** for the hyper-cubic lattice[4]. In spin arrangements, +, − and 0 represent spins of $S_i = 1$, -1 and 0, respectively. When $D < 0$, the perfect 0 ordering occurs in the region of $J' < -1 - 2D/\theta$ (θ: the cordination number), and when $D > 0$, the SQ ordering, which takes two-sublattice structure, occurs in the region of $J' < -1 - D/\theta$. When $D = 0$, the system is energetically degenerated in the region of $J' < -1$ and takes the spin arrangements where the orthogonal-spin pairs (neighboring spin pairs involving at least one spin $S_i = 0$): $(S_i, S_j) = (0, 1), (0, 0), (0, -1)$, are distributed randomly. In the BEG model with $J = 0$ (i.e. $J'/J \to -\infty$) and $D = 0$, the ordered phase appears at finite temperature[5]. Because the frustration between the interactions does not exist, it is considered that the occurrence of this ordered phase is not caused by macroscopic valleys of the free energy, like the hysteresis. In the hexagonal Heisenberg antiferromagnet, the entropy-induced phase transitions occur due to thermal fluctuations (i.e. entropy effect) while the ground state is energetically degenerated[35], and it seems likely that the thermal fluctuations cause the SQ phase.

Appendix II. Finite-size effect

As for the critical relaxation, the dynamic finite-size scaling theory for the order parameter yields a cross-over effect in relation to time region: at $t < t^*$, where t^* is the cross-over time, the bulk-like power-law relaxation takes place, and at $t > t^*$ the finite-size effect is

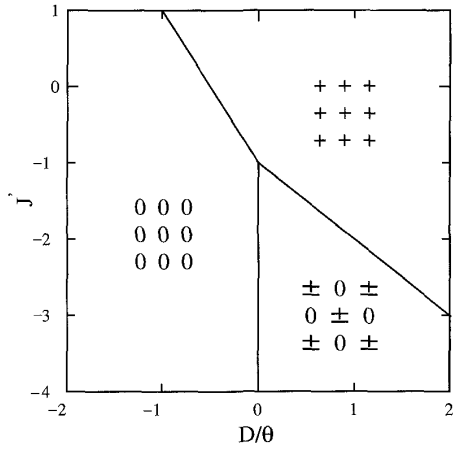

Fig. 11 Ground state phase diagram and spin arrangements in the BEG model on a hypercubic lattice. θ is the coordination number.

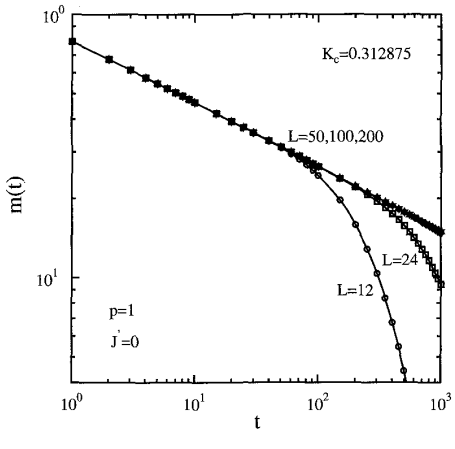

Fig. 12 Time evolution of the order parameter $m(t)$ for $L = 12$, 24, 50, 100 and 200. The simulations are performed at the critical temperature $K_c = 0.312875$ in the pure system ($p = 1$) with $J' = 0$.

observed[26]. **Fig. 12** shows the time evolution of the order parameter $m(t)$ for several linear sizes of lattice: $L = 12$, 24, 50, 100 and 200. The number of bond samples is $N_s = 160$ ($L = 200$), 1600 (100), 8000 (50), 40000 (24) and 200000 (12). The pure system ($p = 1$) with $J' = 0$ is simulated at the critical temperature $K_c = 0.312875$, taken from our measurement (see **Table 1**). It is found that the cross-over time depends on L and becomes larger with the increase of L: the curves for $L = 12$ and $L = 24$ exhibit the power-law behavior only up to $t^* \sim 50$ and $t^* \sim 200$, respectively while the curves for $L = 50$ up to $L = 200$ completely overlap and exhibit the power-law behavior up to $t = 1000$.

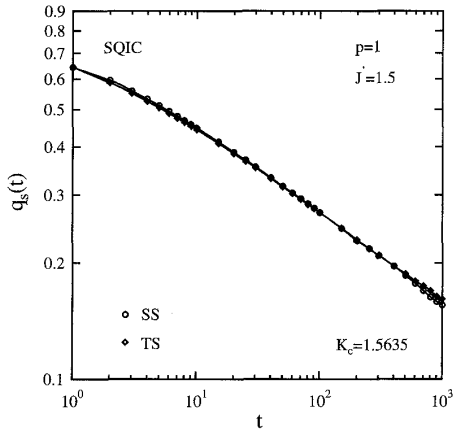

Fig. 13 Time evolution of the order parameter $q_s(t)$ for the two different schemes of selecting spin to be flipped: SS and TS. The simulations are performed at the critical temperature $K_c = 1.5635$ in the pure system ($p = 1$) with $J' = -1.5$.

Appendix III. Sampling scheme

At the stage of selecting the spin to be flipped, we have two different sampling schemes: sequential sampling throughout lattice (SS) and sequential sampling along each of two sublattices (TS). In the FM transition, it is known that an asymptotic power-law relaxation at critical point is not affected by a choice of the sampling procedure[36]. In order to see the influence of the sampling scheme for the case of the SQ phase which takes the two-sublattice structure, the time evolution of the order parameter $q_s(t)$ starting from SQIC, is shown in **Fig. 13**, comparing the two different sampling schemes. The pure system ($p = 1$) with $J' = -1.5$ is simulated at the critical temperature $K_c = 1.5635$, taken from our measurement (see **Table 2**). The linear size of lattice is $L = 100$, and the number of bond samples is $N_s = 160$. It is observed that the curves for the two sampling schemes show the predicted power-law relaxation and coincide without parallel shift.

References

1) M. Blume, V.J. Emery, R.B. Griffiths, Phys. Rev. A 4 (1971) 1071.
2) Y.L. Wang, C. Wentworth, J. Appl. Phys. 61 (1987) 4411.
3) Y.L. Wang, F. Lee, J.D. Kimel, Phys. Rev. B 36 (1987) 8945.
4) K. Kasono, I. Ono, Z. Phys. B 88 (1992) 205.
5) K. Kasono, I. Ono, Z. Phys. B 88 (1992) 213.
6) K. Binder, A.P. Young, Rev. Mod. Phys. 58 (1986) 801.
7) K.H. Fischer, J.A. Hertz, Spin Glasses, Cambridge University Press, Cambridge, 1991.
8) A. Albino Jr, F.D. Nobre, F.A. da Costa, J. Phys. A 12 (2000) 5713.
9) F.A. da Costa, F.D. Nobre, C.S.O. Yokoi, J. Phys. A 30 (1997) 2317.
10) J.J. Arenzon, M. Nicodemi, M. Sellitto, J. de Phys. I 6 (1996) 1143.
11) M. Nicodemi, A. Coniglio, J. Phys. A 30 (1997) L187.
12) G.R. Schreiber, Eur. Phys. J. B 9 (1999) 479.

13) W. Gotze, L. Sjogren, Rep. Prog. Phys. 55 (1992) 241.
14) M.D. Ediger, C.A. Angell, S.R. Nagel, J. Phys. Chem. 100 (1996) 13200.
15) N. Ito, Y. Ozeki, H. Kitatani, J. Phys. Soc. Jpn. 68 (1999) 803.
16) N. Ito, T. Matsuhisa, H. Kitatani, J. Phys. Soc. Jpn. 67 (1998) 1188.
17) Y. Ozeki, N. Ito, J. Phys. A 31 (1998) 5451.
18) Y. Nonomura, J. Phys. Soc. Jpn. 67 (1998) 5.
19) Y. Nonomura, J. Phys. A 31 (1998) 7939.
20) N. Ito, in: D P Landau, K K Mon, H -B Schüttler (Eds.), Computer Simulation Studies in Condensed Matter Physics XI, Springer, Berlin, 1999.
21) N. Ito, K. Ogawa, K. Hukushima, Y. Ozeki, Prog. Theor. Phys. 138 (2000) 555.
22) A. Jaster, J. Mainville, L. Schülke, B. Zheng, J. Phys. A 32 (1999) 1395.
23) N. Ito, K. Hukushima, K. Ogawa, Y. Ozeki, J. Phys. Soc. Jpn. 69 (2000) 1931.
24) K. Ogawa, Y. Ozeki, J. Phys. Soc. Jpn. 69 (2000) 2808.
25) M. Suzuki, Phys. Lett. A 58 (1976) 435.
26) M. Suzuki, Prog. Theor. Phys. 58 (1977) 1142.
27) K. Binder, Z. Phys. B 43 (1981) 119.
28) R.N. Bhatt, A.P. Young, Phys. Rev. B 37 (1988) 5606.
29) N. Kawashima, A.P. Young, Phys. Rev. B 53 (1996) R484.
30) H. Nishimori, Prog. Theor. Phys. 66 (1981) 1169.
31) H. Nishimori, J. Phys. Soc. Jpn. 61 (1992) 1011.
32) H. Nishimori, J. Phys. Soc. Jpn. 55 (1986) 3305.
33) A.B. Harris, J. Phys. C 7 (1974) 1671.
34) Y. Ozeki, H. Nishimori, J. Phys. Soc. Jpn. 56 (1987) 1568.
35) S. Watari, S. Miyashita, H. Shiba, J. Phys. Soc. Jpn. 70 (2001) 532.
36) M. Kikuchi, J. Phys. Soc. Jpn. 55 (1986) 1359.